Homological spanning forest framework for 2D image analysis

Helena Molina-Abril · Pedro Real

Abstract A 2D topology-based digital image processing framework is presented here. This framework consists of the computation of a flexible geometric graph-based structure, starting from a raster representation of a digital image *I*. This structure is called Homological Spanning Forest (HSF for short), and it is built on a cell complex associated to *I*. The HSF framework allows an efficient and accurate topological analysis of regions of interest (ROIs) by using a four-level architecture. By topological analysis, we mean not only the computation of Euler characteristic, genus or Betti numbers, but also advanced computational algebraic topological information derived from homological classification of cycles. An initial HSF representation can be modified to obtain a different one, in which ROIs are almost isolated and ready to be topologically analyzed. The HSF framework is susceptible of being parallelized and generalized to higher dimensions.

1 Introduction

One of the main goals of digital image processing and computer vision is the research and development of flexible and topologically-consistent frameworks for nD image

H. Molina-Abril (✉) · P. Real
Dpto. Matematica Aplicada I, E.T.S.I. Informatica, Universidad de Sevilla,
Avda. Reina Mercedes, s/n 41012 Sevilla, Spain
e-mail: habril@us.es

P. Real
e-mail: real@us.es

⁂ Springer

processing and object recognition. Roughly speaking, topology in a discrete context helps to understand the degree of connectivity of subdivided geometric structures. For subdivided objects, homology is topology measured in terms of linear combinations (called chains) of unit elements or bricks (also called cells), and in terms of a "boundary operator" describing the connectivity dependencies among these bricks. Homology depends on the ring of coefficient and it gives an algebraic answer in terms of formal sums of bricks that have no boundary (for example, closed subdivided curves or surfaces). These sums are called cycles and homology determines a representative cycle for each n-dimensional hole or homology generator the object has (connected components, tunnels, cavities, etc). In this way, homology can be considered as an specification of the contribution of each brick, to the creation of the homology representative cycles.

We present here a $2D$ topology-based digital image processing framework that is built on a graph-based structure, called Homological Spanning Forest (HSF, for short). This framework allows an efficient and complete topological region-of-interest (ROI, for short) analysis (that is to process a single subregion of an image, leaving other regions unchanged). The proposed framework provides a representation that can be used for the development of efficient algorithms to compute analytical, geometrical and topological features of discrete objects.

In order to facilitate the understanding of this idea, we start with an elementary example of a subdivided object. Given a geometric graph G, the homology information in which we are interested can be directly captured by means of a spanning tree T of G. In fact, we transform T into a directed tree T^d by adding arrows to every edge in T, in such a way that at most one arrow comes out from each vertex. Therefore, there will be only one vertex s of G, called sink, from which no arrow comes out. Let us take now the simple example of Fig. 1, drawn on $\mathbb{R}^2$. Let us now interpret an arrow (f, e) in T^d from the vertex f to the vertex e as an elementary "deformation" operation "contracting" in a continuous way the vertex f onto e through the edge (e, f) inside the object. The result of applying (no matter the order we choose) the set of homology-preserving operations $\mathcal{V} = \{(a, f), (b, c), (c, d), (d, e), (f, e)\}$ on G is a reduced (in terms of bricks) subdivided structure consisting of only three bricks: the vertex e, and two loops or "edges" starting and ending at the same common vertex e (in fact, they represent the cycles $\{(c, f), (e, f), (d, e), (c, d)\}$ and $\{(a, b), (a, f), (e, f), (d, e), (c, d), (b, c)\}$ coming from (c, f) and (a, b), respectively).
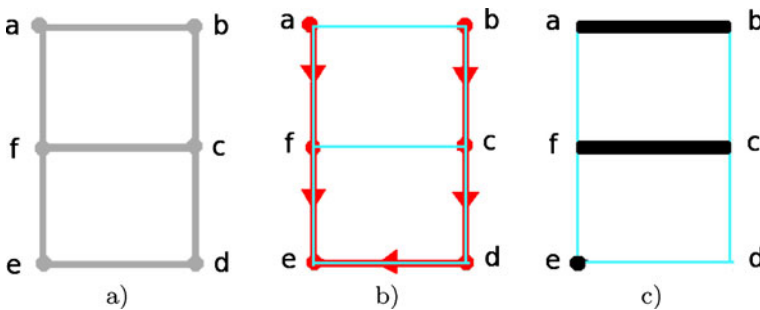

Fig. 1 **a** A geometric graph G drawn on $\mathbb{R}^2$, **b** a directed spanning tree (in *red*) showing a homological "deformation" process and **c** the minimal homological object (in *black*)

The directed spanning tree T^d can be interpreted in dynamical terms, as the way in which the set of vertices of the graph is "collapsed" to a representative vertex of the connected component (in this case, the vertex e in black). These three representative cycles of homology generators (in this case, no matter of the ground ring we use but heavily dependent on the spanning tree T) are determined by the following bricks of G (called *critical*): the edges (c, f), (a, b) belonging to $G \setminus T$, and the sink vertex e belonging to T. Its integer homology groups are one copy of $\mathbb{Z}$ in dimension 0 and two copies in dimension 1. A Homological Spanning Forest or HSF representation $\mathcal{F}(G)$ for the subdivided geometric structure G is the set of coordinate-based trees $\mathcal{F}(G) = \{T^d, T_1, T_2\}$, where T_1 and T_2 are trees composed by only one "vertex": the original edges (a, b) and (c, f) respectively.

This "homological representation" has some properties that we will study later under a more general, rigorous and formal mathematical context:

(a) *Non-uniqueness*: it is not unique and strongly depends on how the set of bricks is managed in order to obtain a minimal homological expression.
(b) *Local Transformability*: a global HSF representation can be transformed into a different one by using local combinatorial operations.
(c) *Geometric Acuity*: the use of coordinate-based trees allows to capture the geometry of the original object (each node is specified by an ordered pair of integer coordinates with respect to the square grid of the initial image).
(d) *Topological Acuity*: it suitably encodes advanced topological features (Euler characteristic, Betti numbers, classification of cycles, determining the contractibility and transformability of cycles inside the object, numerical invariants related to cohomology algebra, cohomology operations, ...), due to the fact that the HSF forest can be automatically rewritten in algebraic terms (with coefficients in a field) as a chain homotopy operator determining a strong relationship at chain level (formal sums of bricks) between the geometric object G and its minimal homological expression; that is, a chain homotopy equivalence.
(e) *Reusability*: a HSF representation of a subgraph G' of G can be derived automatically from a previously computed HSF representation of G.

We work in this paper with HSF structures within the context of discrete (raster) 2D images. In this highly structured setting, preference will be given to an ambiance-based digital image processing rather than to an object-based one. Assuming that the ambiance carrier (cell complex) of a digital image is topologically trivial (i.e., it has the homology of a point), we extend here to dimension two the homological meaning (in terms of cell collapse-like operations) of the spanning tree notion over a graph. In this way, such a combinatorial HSF scaffolding in which the values of the pixels of a digital image I become the weights for the respective 0-cells fully represent I from a topological point of view.

Referring to a whole image I of dimension $n \times m$, its associated HSF set of coordinated-based direct trees can be, initially, independent of the pixel contents of the digital image I. A HSF representation $\mathcal{F}(I)$ leans on an common underlying continuous analogous for all the images. In 2D, it is a finite cell complex $K_{m,n}$ that is collapsible to a cell (more precisely, cubical) complex version of the Euclidean plane P, whose 0-cells are the pixels of I, the 1-cells describe the relationships between 4-adjacent pixels in terms of straight lines, and the closure of 2-cell are squares formed

by four pixels mutually 8-adjacent. Although this framework works for any different discrete type of adjacency between pixels (8, 6 or 4 connectedness), we focus here on 8-connectedness. In this case, $K_{n,m}$ is a cell complex with elementary "pockets" (see Fig. 9). Now, starting from a HSF-representation of a digital image, there is an efficient way to "deform" it to a new one, and to isolate ROIs, in order to, for example, analyze further topological features on them. Let us emphasize that these constructions can be built in a parallel setting.

There are in the literature an enormous number of papers dealing with techniques that reduce the structural shape of a $2D$ region to a graph (skeletons, shock graph, cut-graph methods, combinatorial maps, pyramids, ...) (see for example [11, 31, 32]). A substantial minor number of papers handle a cell complex based representation of a $2D$ digital image (see for instance [2, 24, 28, 29]).

Our combinatorial HSF framework for 2D digital image processing can be classified as a hybrid method that is based on the description of homological information about cell complexes in terms of directed graphs. The object modeling in this context can be considered as a combinatorial refinement of the AT-model method (algebraic-topological method) developed in papers [16–18]. The AT-model is based in the description of homology in terms of chain homotopies. This idea is not new (comes back to the Eilenberg–MacLane work on Algebraic Topology [10]) and has been developed in algebraic-topological methods like Effective Homology [37, 40] and Homological Perturbation Theory [20] and in the discrete settings in Discrete Morse [13] and AT-model [15, 33] theories. For example, in Discrete Morse Theory, the HSF structure can be specified as an appropriate graph description of an optimal discrete gradient vector field.

The paper is structured as follows: We begin with recalling basic definitions and results in Section 2. In the following section, we give an introductory idea of the HSF technique for finite cell complexes. In Section 4 the proposed framework for discrete 2D images is detailed. Homology and cohomology computation based on the HSF technique are developed in Section 5. We present a parallel homology-based processing using the HSF framework in Section 6, and conclude the paper in Section 7.

Most of the figures of $2D$ digital images in the paper have been created using the software developed in [38].

2 Preliminaries

In this section, we introduce some useful concepts for the understanding of the paper.

A *digital image I* is a function defined on a discrete set D in $\mathbb{R}^n$ (carrier of the image) onto a discrete set V in $\mathbb{R}$ (usually $\{0, 1\}$ for binary images or $\{0, 1, \ldots, 255\}$ for gray-level images). The carrier of I is usually a subset of a uniform regular grid defining $\mathbb{Z}^2$. An object of interest $O \subset D$ in a digital image $I : D \to V$, has as image support function $w : D \to \{0, 1\}$, which assigns the value 1 to any pixel of O, whereas each pixel of $O^c = D \backslash O$ has the value 0 (O^c is named the background).

Let us now recall some definitions from algebraic topology.

A *topological space* is a set of points X with a definition for the open subsets of X, usually called neighborhoods. Two topological spaces X and Y are considered equivalent if there exist a homeomorphism between them, i.e., a continuous bijective function $f : X \to Y$ whose inverse is continuous.

The goal of a topological map is to partition a topological space up into regions that are homeomorphic to open balls (see [5, 42]). More formally, for $p \geq 1$ define $\mathbb{B}^p = \{x \in \mathbb{R}^p : |x| < 1\}$, $\overline{\mathbb{B}}^p = \{x \in \mathbb{R}^p : |x| \leq 1\}$, $\mathbb{S}^p = \{x \in \mathbb{R}^{p+1} : |x| = 1\}$.

A space homeomorphic to $\mathbb{B}^p$ is called an *open p-cell*, a space homeomorphic to $\overline{\mathbb{B}}^p$ is called a *closed p-cell*, and a space homeomorphic to $\mathbb{S}^p$ is called a *p-sphere*. By convention we say that single points are both open and closed 0-cells. A partition of a space into open cells is called a *CW-complex*. Recall that a p-dimensional (finite, normal, homogeneous) CW-complex K is a pair $(X, \{K_i\}_{i=0}^p)$ where X is a Hausdorff space and $\{K_i\}_{i=0}^p$ is a finite partition of X into open cells such that:

– the set K_i is the set of all open *i*-cells with $0 \leq i \leq p$.
– for every open *p*-cell, σ, there is a continuous map $h_\sigma : \overline{B}^p \to X$ whose restriction to B^p is a homeomorphism onto σ and whose restriction to S^{p-1}, called *boundary of σ* and denoted $\partial\sigma$, is the union of open cells in K of dimension less than p. The space $h_\sigma(\overline{B}^p) = \overline{\sigma}$ is called *closure of the open cell σ* and $\overline{\sigma} = \sigma \cup \partial\sigma$. In addition it is required that every open cell σ is either a *p*-cell or is in the boundary of a *p*-cell. To indicate relationships between cells, we write $\tau > \sigma$ (or $\sigma < \tau$) and we say that σ is a face of τ if $\sigma \neq \tau$ and $\sigma \subset \overline{\tau}$. We write $\tau \geq \sigma$ if either $\tau \geq \sigma$ or $\tau > \sigma$.

The *p-skeleton* $K(p)$ of K is the set of all *k*-cell $\bigcup_{r=0}^p K_r$, with $0 \leq k \leq p$. If all the cells of K are convex sets of the Euclidean *p*-dimensional space, then each cell can be represented by a its a new point interior to each cell (commonly, its barycenter) and K is called convex cell complex. Simplicial, cubical and some polyhedral complexes are special cases of convex cell complexes. All the complexes in this paper are convex cell complexes embedded into the Euclidean *p*-dimensional space.

In this paper the considered ring of coefficients Λ is the finite field $\mathbb{Z}/2\mathbb{Z} = \{0, 1\}$, but all the results are valid for any commutative field (another finite field, the rational numbers, the real numbers,...). Let $\{x_1, x_2, ..., x_n\}$ be a finite set of symbols. The finite vector space of formal linear combinations $\lambda_1 x_1 + \lambda_2 x_2 + \ldots + \lambda_n x_n$, with $\lambda_i \in \Lambda$, is denoted by $\Lambda[x_1, \ldots, x_n]$.

Given a cell complex K, one can define, for each dimension q, the chain vector space $C(K)_q$ whose elements, called *q-chain*, are linear combinations of cells of dimension q (q-cells). Then, the *chain complex* $\mathcal{C}(K)$ canonically associated to the finite cell complex K is a differential graded vector space given by a couple $(C(K), \partial)$, where $C(K) = \{C(K)_q\}_{0 \leq q \leq d}$ is a finite sequence of chain vector spaces $C(K)_q$, and the *differential* (bounding relation) $\partial = \{\partial_q\}_{0 \leq q \leq d}$ is a sequence of homomorphisms $\partial_q : C(K)_q \to C(K)_{q-1}$, such that the composition of any two consecutive maps is zero: $\partial_q \circ \partial_{q-1} = 0$ for all $0 < q \leq d$ (and $\partial_0 \equiv 0$).

For the convex cell complexes and the coefficients ring considered in this paper, the differential for an open *p*-cell σ can be automatically deduced from its boundary. If $\tau_1, \ldots, \tau_r$ are the open $(p-1)$-cells belonging to the the boundary $\partial\sigma$, the differential for σ is the sum $\tau_1 + \ldots + \tau_r$.

A *q*-chain $c \in \mathcal{C}(K)_q$ is called a *q-cycle* if $\partial_q c = 0$. If $c = \partial_{q+1}b$ for some $b \in \mathcal{C}(K)_{q+1}$ then c is called a *q-boundary*. Denote the vector space of *q*-cycles and *q*-boundaries by Z_q and B_q respectively. Roughly speaking, the idea of homology is to analyze the degree of connectivity of cell complexes using formal sums of cells. Thanks to the nilpotency property of ∂, it is true that $Z_q \subseteq B_q$ for all $q \geq 0$. Define the qth *homology group* of the cell complex K (or equivalently, of the chain complex

$\mathcal{C}(K))$ to be the quotient group Z_q/B_q. We say that c is a *representative q-cycle* of the homology generator $c + B_q$.

Elementary chain homotopy operators (that is, linear maps $\phi : C(K)_* \to C(K)_{*+1}$) acting on a cell complex K can be used to describe the process of homology computation for K at chain complex level. In the case of coefficients on a field, it has been proved (see [15, 22, 33]) that the whole homology computation process can be exclusively specified by the exhaustive use of these operations. In that case, they are a chain homotopy equivalence version of the classical cell collapsing operation (see, for example, [4]).

We interpret now some elementary notions of Discrete Morse Theory [13, 14] in terms of chain homotopy equivalences.

Let K be a finite cell complex and σ a cell of K of dimension t ($t \in \{1, 2\}$). If $u_1, \ldots, u_r$ ($r \in N$) are the $(t-1)$-cells which form the boundary $\partial(\sigma)$ of σ, let us take $\phi_{u_i,\sigma} : \mathbb{Z}/2\mathbb{Z}[K] \to \mathbb{Z}/2\mathbb{Z}[K]$ defined by $\phi(u_i) = \sigma$ and zero elsewhere. The map $\phi_{u_i,\sigma}$ is called *cell homology collapsing* and is a *chain homotopy operator* satisfying the properties: (a) $\phi_{u_i,\sigma} \circ \phi_{u_i,\sigma} = 0$, (2-nilpotency condition) and (b) $\phi_{u_i,\sigma} \circ \partial \circ \phi_{u_i,\sigma} = \phi_{u_i,\sigma}$ (chain contraction condition). In fact, this map generates the following chain homotopy equivalence between differential graded vector spaces (also called a chain contraction in [10]):

$$(f_{u_i,\sigma}, incl, \phi_{u_i,\sigma}) : (\mathcal{C}(K) = \mathbb{Z}/2\mathbb{Z}[K], \partial) \to f(\mathcal{C}(K)) = (f(\mathcal{C}(K)), \partial') \qquad (1)$$

where $f_{u_i,\sigma} : \mathcal{C}(K) \to f(\mathcal{C}(K))$ is the map $f_{u_i,\sigma} = 1_{(C(K))} + \partial \circ \phi_{u_i,\sigma} + \phi_{u_i,\sigma} \circ \partial$ (being $1_{C(K)} : \mathcal{C}(K) \to \mathcal{C}(K)$ the identity function on $C(K)$), $f(\mathcal{C}(K)) = \{f(c) \ / \ c \in C(K)\} \subset C(K)$, $incl : f(\mathcal{C}(K)) \to C(K)$ is the linear operator defined by $i(z) = z$, $\forall z \in f(\mathcal{C}(K))$ and $\partial' : f(\mathcal{C}(K))_q \to f(\mathcal{C}(K))_{q-1}$ is the differential defined by $\partial'(f(c)) = f(\partial(c)) = (\partial + \partial \circ \phi_{u_i,\sigma} \circ \partial)(c)$. Concretely, $f(u_i) = \sum_{k \neq i} u_k$, $f(\sigma) = 0$ and if $\sigma' \in C_t(K)$ and $\partial(\sigma') = u_i + \ldots$, then $f(\sigma') = \sigma + \sigma'$ and $\partial'(f(\sigma')) = \partial(\sigma + \sigma')$. Finally, f is the identity map and $\partial' = \partial$ for the rest of cells. In Fig. 2, a cell homology collapsing operator (represented with a red arrow) and the result after its application are shown.

It is straightforward to prove the following properties (guaranteeing in this way that $c_{u_i,\sigma} = (f_{u_i,\sigma}, incl, \phi_{u_i,\sigma})$ is a chain contraction):

(a) $1_{C(K)} + incl \circ \ f_{u_i,\sigma} = \partial \circ \phi_{u_i,\sigma} + \phi_{u_i,\sigma} \circ \partial$
(b) $f_{u_i,\sigma} \ \circ incl = 1_{f(C(K))}$
(c) $\phi_{u_i,\sigma} \ \circ incl = 0 = f_{u_i,\sigma} \ \circ \phi_{u_i,\sigma}$
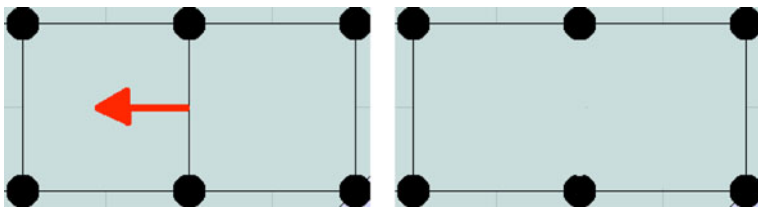

Fig. 2 A cell homology collapsing and the resulting cell complex

In particular, these properties mean that the homology groups of the differential graded vector spaces $\mathcal{C}(K)$ and $f(\mathcal{C}(K))$ are isomorphic. If u_i belongs to the boundary of only one cell σ ($\{u_i, \sigma\}$ is also called *a free pair*), then $f(\mathcal{C}(K)) = (\mathbb{Z}/2\mathbb{Z}[K \setminus \{u_i, \sigma\}], \partial)$ and this chain contraction is a classical cell collapse (see Fig. 3 for an example).

A finite cell complex X collapses onto Y if there is a sequence of cell complexes $< X_0, X_1, \ldots, X_\ell >$ (also called *cell collapse sequence*) such that $X_0 = X$ and $X_\ell = Y$, and there is an elementary collapse from X_{i-1} to X_i, for all $i = 1, \ldots, \ell$. A cell complex $Y \subset X$ is called a *strong deformation retract* if the cell complex X collapses onto Y. A cell complex X is called *collapsible* if it collapses onto a cell complex $X\{*\}$ made of a single point. In particular, a collapsible cell complex is acyclic, that is, having the same homology groups as a single point. The elementary collapse operation from X_{i-1} to X_i is specified by a free pair $\{u, \sigma\}$ in X_{i-1}. Both u and σ also belong to X_0, due to the fact that at each step, free pairs are considered. In this way, we can reinterpret the notion of cell collapse sequence at chain complex level as a sum of chain contractions. This homotopy equivalence is determined by the chain homotopy operator such that $\phi(u) = \sigma$, for all the involved free pairs $\{u, \sigma\}$. In the next section, we determine a method for dealing with elementary chain contractions $c_{u,\sigma}$, where $\{u, \sigma\}$ runs over a discrete vector field $\mathcal{V}$ for determining the global homological structure of an acyclic cell complex in combinatorial terms.

The following notions from Discrete Morse Theory [14] are essential in the sequel:

A *discrete vector field* $\mathcal{V}$ defined on a cell complex K is a pairwise disjoint collection of sets of two incident cells $\{\alpha^{(p)} < \beta^{(p+1)}\}$.

An *integral path* γ for a discrete vector field $\mathcal{V}$ is an alternating sequence of cells $\alpha_0^{(p)}, \beta_0^{(p\pm 1)}, \alpha_1^{(p)}, \beta_1^{(p\pm 1)}, \alpha_2^{(p)}, \ldots$, such that for each pair of consecutive simplexes, one is a maximal face of the other, and the following condition is satisfied: one of the couples $\{\alpha_i^{(p)}, \beta_i^{(p+1)}\}$ or $\{\beta_i^{(p\pm 1)}, \alpha_{i+1}^{(p)}\}$ belongs to $\mathcal{V}$, $\forall i \geq 0$. If the final simplex in the path γ above is $\alpha_r^{(p)}$, then we say that γ has length r. If it ends with $\beta_r^{(p\pm 1)}$ then we say that γ has length $r\frac{1}{2}$. If the cells b_i of the path γ are of dimension $p+1$ and it has length $r\frac{1}{2}$, the integral path γ is called *upper integral path*.

An integral path is non trivial and closed if $r \geq 1$ and the first and last cells in the sequence are the same. A *discrete gradient vector field* is a discrete vector field with no closed integral path.

A cell α is a *critical cell* of $\mathcal{V}$ if it is not paired with any other cell in $\mathcal{V}$. The number of critical cells depends on the discrete gradient vector field considered. A *gradient vector field is optimal* if it has the minimum possible number of critical cells. Forman
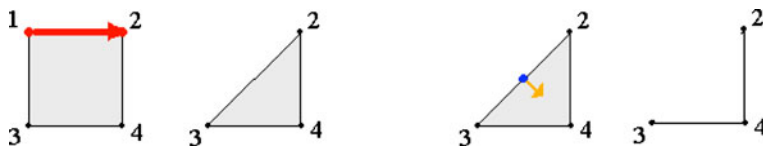

Fig. 3 A cell complex and the resulting cell complex after applying the chain homotopy $\phi(\langle 1 \rangle) = \langle 1, 2 \rangle$ (on the *left*) and a cell complex and the result after applying $\phi(\langle 1, 2 \rangle) = \langle 1, 2, 3 \rangle$ (on the *right*)

proved that the topology of a discrete manifold is related to these critical elements, mimicking the results of Morse in the smooth case.

3 HSF technique for finite cell complexes

In this section, we extract the homological nature of a HSF structure for a finite cell complex, which is half-way between the combinatorial notion of an optimal gradient vector field (Discrete Morse Theory) and the classical algebraic concept of chain contraction (Effective Homology Theory) or even the less elaborate abstraction of a chain homotopy operator (AT-model theory).

In Fig. 1, it is shown that the spanning tree together with the two critical bricks can be seen as a non-redundant structure $M(G)$ which combinatorially represents the geometric graph G. There is a strong algebraic relationship between $M(G)$ and G that is described by means of a chain contraction between them with a chain homotopy operator specified by the HSF structure. Denoting by $\mathbb{Z}/2\mathbb{Z}[G]$ the graded vector space formed by the finite linear combinations of 0-cells and 1-cells of G, we can formalize this chain homotopy operator:

$$\phi_M : \mathbb{Z}/2\mathbb{Z}[G] \to \mathbb{Z}/2\mathbb{Z}[G] \tag{2}$$

with $\phi_M(a) = (a, f) + (f, e)$, $\phi_M(b) = (b, c) + (c, d) + (d, e)$ and, for the rest of vertices, $\phi_M(x)$ is the sum of arrows of the directed path from x to e following the "maximal paths" $\phi_M(a)$ or $\phi_M(b)$. Concerning the vertex e, $\phi_M(e) = 0$. The evaluation of ϕ_M on each of the edges of G is zero.

Using ϕ_M, the following operators can be defined:

1. *The flow, defined as* $f_M = \mathbf{1} + \phi_M \circ \partial + \partial \circ \phi_M : \mathbb{Z}/2\mathbb{Z}[G] \to \mathbb{Z}/2\mathbb{Z}[G]$, *where* $\mathbf{1}$ *and* ∂ *are functions from* $\mathbb{Z}/2\mathbb{Z}[G]$ *to* $\mathbb{Z}/2\mathbb{Z}[G]$ *denoting the identity and the boundary operator of the graph cell complex* G, *respectively.*
2. *The inclusion operator incl:* $\mathbb{Z}/2\mathbb{Z}[C_0, C_1, C_2] \to \mathbb{Z}/2\mathbb{Z}[G]$, *where* C_i ($i \in \{0, 1, 2\}$) *are the homology representative cycles.*

In Fig. 1, $f_M(x) = \{C_0 = e\}$ for each vertex x of G and $f_M((x, y)) = 0$ for each edge (x, y) in the spanning tree T. The flow of the critical edges (a, b) and (f, c) are, respectively the cycles $C_1 = (a, b) + (b, c) + (c, d) + (e, f) + (f, a)$ and $C_2 = (c, f) + (c, d) + (d, e) + (e, f)$.

Therefore, under these conditions, any cell c of G can be obtained as a sum of a homology representative cycle C_i ($i \in \{0, 1, 2\}$) and the homologically inessential linear combination $(\partial \circ \phi_M + \phi_M \circ \partial)(c)$. The cycles C_i ($i \in \{0, 1, 2\}$) are invariant linear combinations of cells through the flow.

In other words, the triple $(f_M, incl, \phi_M)$ is a chain contraction from the chain complex $C(G)$ to $M(G) = \mathbb{Z}/2\mathbb{Z}[C_0, C_1, C_2]$, which is entirely determined by the chain homotopy operator ϕ_M.

For general and higher dimensional cell complexes, the HSF method is more complicated and needs more explanation (see, for example [35]). We first give the definition of HSF structure on a general finite cell complex and, later, we focus on the two-dimensional case, by specifying a priori an optimal gradient vector field on it, and to cell complexes embedded in a regular Cartesian grid (considering this last as a cell complex).

Definition 1 Let K be a finite cell complex. A HSF representation $\mathcal{F}$ of K is a set of coordinate-based directed trees $\mathcal{F} = \{T_1(\mathcal{F}), T_2(\mathcal{F}), \dots, T_r(\mathcal{F})\}$ (for some positive integer r) satisfying the following conditions:

(a) Every convex cell of K is a vertex of only one of the trees of $\mathcal{F}$ and it is represented by its barycenter.
(b) The vertices of a tree $T_i(\mathcal{F}) \in \mathcal{F}$ ($i = 0, \dots p$) are either p-cells (called *primary vertices of T_i*) or $(p+1)$-cells (called *secondary vertices of T_i*). The directed edges of $T_i(\mathcal{F})$ are either upwards $\mathcal{F}$-arrows from a p-cell $\alpha^{(p)}$ to a $(p+1)$-cell $\beta^{(p+1)}$ (from which $\alpha^{(p)}$ is boundary), or downwards $\mathcal{F}$-arrows from a $(p+1)$-cell $\beta^{(p+1)}$ to one of its boundary p-cell $\alpha^{(p)}$. T_i is called a p-tree of $\mathcal{F}$. T_i can have no directed edges and, in this case, it is a trivial tree with only one vertex. Each p-tree T_i has at least one leave that is a p-cell. The upwards $\mathcal{F}$-arrows determine a discrete vector field $\mathcal{V}(\mathcal{F})$ on K.
(c) The following equalities hold:

$$\phi(\mathcal{F}) \circ \partial \circ \phi(\mathcal{F}) = \phi(\mathcal{F}) \quad \text{and} \quad \partial \circ \phi(\mathcal{F}) \circ \partial = \partial.$$

where ∂ is the differential of K and $\phi(\mathcal{F}) : C_*(K) \to C_{*+1}(K)$, called chain homotopy operator associated to $\mathcal{F}$, is defined by: $\phi(\mathcal{F})(\sigma^{(p)})$ is 0 if $\sigma^{(p)}$ is a p-cell belonging to a $(p-1)$-tree of $\mathcal{F}$; if $\sigma^{(p)}$ is a vertex of a p-tree T of $\mathcal{F}$, then $\phi(\mathcal{F})(\sigma^{(p)}) = \Sigma_i(a_i \bmod 2)\beta_i^{(p+1)}$, where $\beta_i^{(p+1)}$ runs over all the $(p+1)$-cells of T and a_i is the number of upper integral $\mathcal{V}(\mathcal{F})$-paths from $\sigma^{(p)}$ to $\beta_i^{(p+1)}$.

In any HSF-representation of K, if exists, its 0-dimensional homological trees specify (not considering the arrows) a barycentric subdivision of a spanning forest of the 1-dimensional skeleton $K^{(1)}$ of K. In some way, this decomposition method can be seen as a "natural" extension to higher dimension of the graph-based techniques for computing the spanning forest of a graph complex and its corresponding zero and one dimensional homology groups. For that reason, we have named this decomposition "Homological Spanning Forest".

As we later prove, there exists such a tree-based structure in digital context. We propose here to calculate HSF strutures for digital objects by means of "deformations" of HSF structures on the ambiance space.

Let K be a finite cell complex such that a cell complex version of a finite regular Cartesian grid is a strong deformation retract of K. From now on, we name such type of space as ASDR (Acyclic Strong Deformation Retract) cell complex. Let $\mathcal{V}$ be an optimal discrete gradient vector field installed on K. Therefore, K is homologically null and all the cells of K are paired by $\mathcal{V}$, excepting a 0-cell s called *sink* of $\mathcal{V}$. In fact, s is a representative cycle of the zero dimensional homology group of K and the chain contraction generated by $\phi_{\mathcal{V}}$ connects the chain complex canonically associated to K with $\mathbb{Z}/2\mathbb{Z}[s]$. In these conditions, K can be "decomposed" into a HSF structure. Moreover, in this case, due to the fact that the context of ASDR cell complexes is highly structured and that the vertices of the HSF structure are convex cells determined by their barycenter, we can talk about HSF representation of digital objects.

In order to prove this result, we take advantage of the algebraic technique of Homological Perturbation Theory [20, 21] applied to the discrete gradient vector field $\phi_{\mathcal{V}}$. This idea has already been exploited in a more general setting in the paper of Romero-Sergeraert [37] for establishing an strong interplay between Effective

Homology and Discrete Morse Theories. In that paper, starting from an optimal gradient vector field on a general finite cell complex, a chain contraction is determined using homological perturbation. Focusing on the chain homotopy operator of this last chain homotopy equivalence, we here give a proof of its graph-based nature.

Lemma 1 [37] *Let K be an ASDR cell complex, $\mathcal{C}(K)$ be its corresponding chain complex and $\phi_{\mathcal{V}}$ be the chain homotopy operator associated to an optimal discrete gradient vector field $\mathcal{V}$. Let s be the sink of $\mathcal{V}$. Then, it is possible to construct the following chain contraction $(f_{\mathcal{V}}, g_{\mathcal{V}}, \phi_{\mathcal{V}})$ from $(C(K), \partial')$ to $(\mathbb{Z}/2\mathbb{Z}[s], \mathbf{0})$, such that the differential $\partial_{\mathcal{V}} : C_*(K) \to C_{*-1}(K)$ is defined by $\partial_{\mathcal{V}}(\sigma) = v_{\sigma}$ where $(v_{\sigma}, \sigma) \in \mathcal{V}$ and the differential $\mathbf{0} : \mathbb{Z}/2\mathbb{Z}[s] \to \mathbb{Z}/2\mathbb{Z}[s]$ is defined by $\mathbf{0}(s) = 0$. The formulae for $f_{\mathcal{V}}$ and $g_{\mathcal{V}}$ are the following ones:*

$$f_{\mathcal{V}} = \mathbf{1} + \partial_{\mathcal{V}} \circ \phi_{\mathcal{V}} + \phi_{\mathcal{V}} \circ \partial_{\mathcal{V}}$$

$$g_{\mathcal{V}}(s) = s$$

Romero and Sergeraert apply the differential perturbation technique to the chain contraction $(f_{\mathcal{V}}, g_{\mathcal{V}}, \phi_{\mathcal{V}})$ from $(C(K), \partial_{\mathcal{V}})$ to $\mathbb{Z}/2\mathbb{Z}[s]$, using as differential perturbation $\delta = \partial - \partial_{\mathcal{V}}$, in order to deduce a true chain contraction $(f_{\mathcal{V}}^{\delta}, g_{\mathcal{V}}^{\delta}, \phi_{\mathcal{V}}^{\delta})$ connecting $C(K)$ (with the original boundary operator) with its homology.

We focus our interest here in the new chain homotopy operator $\phi_{\delta} = \phi_{\mathcal{V}} + \phi_{\mathcal{V}} \circ \delta \circ \phi_{\mathcal{V}} + \ldots + \phi_{\mathcal{V}} \circ \delta \circ \phi_{\mathcal{V}} \circ \delta \circ \phi_{\mathcal{V}} + \ldots$ to derive a graph structure HSF from it.

For a q-cell a $(q = 1, 2)$, $\delta(a) = u_1 + \ldots + u_t$, such that each u_i is not paired with a by means of $\mathcal{V}$.

For a q-cell a_0, the value $\phi_{\delta}(a_0)$ is a sum of $(1 + r_2 + \ldots + r_t)$ $(q + 1)$-cells $\phi(a_0) = b_{0,1}$, $\phi \circ \delta \circ \phi(a_0) = b_{1,2} + \ldots + b_{r_2,2}$, $\ldots$, $(\phi \circ \delta)^{t-1} \circ \phi(a_0) = b_{1,t} + \ldots + b_{r_t,t}$. In fact, $\delta \circ \phi(a_0) = a_{1,2} + \ldots + a_{r_2,2}$, with $\phi_{\mathcal{V}}(a_{1,2}) = b_{1,2}, \ldots, \phi_{\mathcal{V}}(a_{r_2,2}) = b_{r_2,2}$. Analogously, $(\delta \circ \phi)^{t-1}(a_0) = a_{1,t} + \ldots + a_{r_t,t}$, with $\phi_{\mathcal{V}}(a_{1,t}) = b_{1,t}, \ldots, \phi_{\mathcal{V}}(a_{r_t,t}) = b_{r_t,t}$. On the other hand, $\phi_{\delta}(C(K))$ is an acyclic graded vector space. It is combinatorial in the sense that it admits a basis formed by cells of K. If $\phi_{\mathcal{V}}(a) = b$, then b also belongs to $\phi_{\delta}(C(K))$. Let us note that $\phi_{\delta}(a) = \phi_{\mathcal{V}}(a) + \phi_{\delta}(\delta(b))$ and therefore $b = \phi_{\delta}(a) - \phi_{\delta}(\delta(b))$.

With all these results at hand, $\phi_{\delta}(a_0) = b_{0,1} + b_{1,2} + \ldots + b_{r_2,2} + \ldots + b_{1,t} + \ldots b_{r_t,t}$ can also be expressed as a directed tree $T_{\mathcal{V}, a_0}$, having as vertices $V(T_{\mathcal{V}}, a_0)$ all the p and $(p + 1)$-cells

$$\{a_0 = a_{0,1}, b_{0,1}, a_{1,2}, \ldots, a_{r_2,2}, b_{1,2}, \ldots, b_{r_2,2}, \ldots, a_{1,t}, \ldots, a_{r_t,t}, b_{1,t}, \ldots b_{r_t,t}\},$$

previously described. The set of edges $E(T_{\mathcal{V}, a_0})$ is formed by arrows from $a_{i,j}$ to $b_{i,j}$, $\forall i, j$, and from a $(q + 1)$-cell $b_{i,j}$ with a q-cell $a_{k,\ell}$ belonging to its boundary. Moreover, any path starting from a_0 and finishing in a $(p + 1)$-cell is an upper integral path for $\mathcal{V}$. In fact, $\{a_0\} \cup \phi_{\delta}(a_0)$ is homotopy equivalent to $T_{\mathcal{V}, a_0}$ (see Fig. 4).

It can occur that there are two cells a, a', with $a \neq a'$, for which $V(T_{\mathcal{V}, a}) \cap V(T_{\mathcal{V}, a'}) \neq \emptyset$. In this case, the union of the corresponding associated trees is again a new tree containing the previous ones. Finally, from this data it is immediate to establish a HSF structure accomplishing all the conditions of Definition 1.

In Fig. 5, an optimal gradient vector field for a cubical complex K and the upper integral path starting from the edge e are shown. In fact, this path can also be seen as sums of cells $\phi_{\delta}(e)$. The 2-cells forming the sum $\phi_{\delta}(e)$ are represented by blue thick

Fig. 4 HSF representation in which the sum of 2-cells $\phi(e)$ is colored in *white*. Its associated homological tree $T_{V,e}$ is colored in *black*
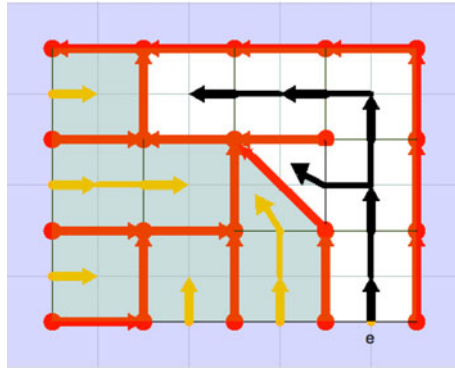

Fig. 5 An optimal gradient vector field for a cubical complex and the upper integral path starting from the edge e. The homological tree $T_{V,v}$, or in this case $\phi(v)$, is colored in *black*
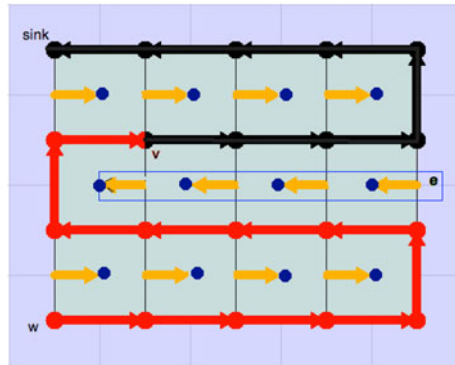

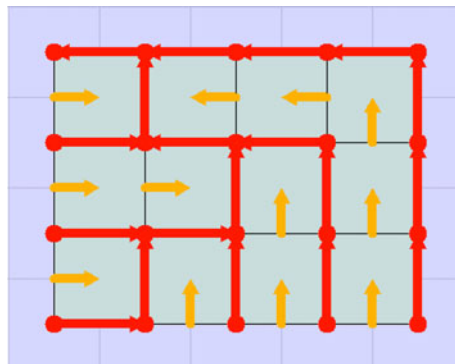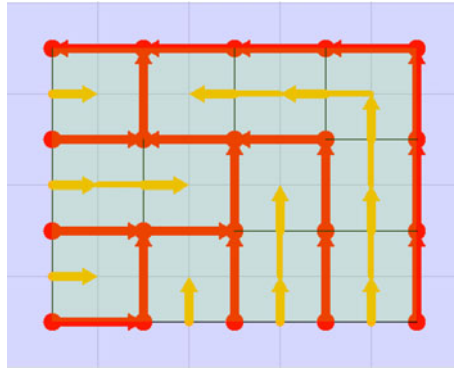**Fig. 6** An optimal gradient vector field for a cubical complex

Fig. 7 HSF representation
where the tree 0-dimensional
tree is colored in *red* and the
1-dimensional trees in *yellow*

points. Then, it is possible to construct a HSF structure on the ASDR cell complex
K from $\phi_\delta(C(K))$.

In Fig. 6, an optimal discrete gradient vector field is described for the acyclic
cubical complex K. In Fig. 7, a HSF representation of K is shown.

Theorem 1 *Let K be a finite 2-dimensional ASDR cell complex and suppose that
there is an optimal discrete gradient vector field $\mathcal{V}$ on it. Then, there is a HSF structure
$\mathcal{F}^{\mathcal{V}}$ uniquely associated to $\mathcal{V}$. Reciprocally, a HSF graph structure on K produces in
a natural way an optimal discrete gradient vector field. Moreover, one of the discrete
gradient vector fields associated to a HSF structure coming from an initial optimal
discrete gradient vector field $\mathcal{V}$ is $\mathcal{V}$ itself.*

The first part of the previous theorem has already been proved. Now, a HSF
configuration on a general cell complex generates discrete gradient vector fields,
which can be not optimal. The acyclicity of an ASDR cell complex allow to guarantee
the optimality. The arrows from a i-cell to an $(i + 1)$-cell ($i = 0, 1$) of the HSF
forest produce the corresponding vectors in the gradient vector field. This strong
relationship between these two important notions for ASDR cell complexes supports
the existence of a homology-based digital image processing framework in this setting.

In the next section, we also confirm a good behavior of the HSF configurations un-
der local transformations within a ASDR cell complex. We also highlight the power
of this representation for advanced topological sequential or parallel computation.

4 HSF and 2D digital image processing

Throughout this section, we describe the functional architecture of our 2D digital
image processing framework. This schema has four levels: Device, Logical or Cellu-
lar, Conceptual and Continuous Level. In the Device Level we represent the objects
in a computer screen, that is, as digital images. In this paper, this representation is
exclusively restricted to that of a digital image based on square pixels. The carrier
of all the digital images is defined on the planar cartesian grid. The pixels of the
digital image are the vertices of the grid. We mainly use the raster representation
of images at Device Level. The Logical or Cellular Level models the connectivity

relationships among pixels using a cell complex structure. The only restriction is that the ambiance cell complex must be an ASDR complex. We have demonstrated in the previous section that for this kind of subdivided spaces, optimal gradient vector fields can be identified with HSF representations (see Theorem 1). The Conceptual Level deals with the homological information of the previous cell complex codified in terms of coordinated-based direct acyclic graphs or "homological spanning trees". Finally, the Continuous Level is used to find a continuous solution. We follow the general organization of the digital framework of [3], integrating essentially new proposals for the logical and conceptual levels.

The models for the Device and Continuous Levels are well known and do not need more explanation. We focus our interest on the Cellular and Conceptual Levels of the framework. It is in these levels of digital content where the HSF graph-based structure becomes a true geo-topological (geometric and topological) representation of digital objects. The representation of the vertices of the HSF in terms of the coordinates (in $\mathbb{R}^2$) of the barycenter of the cells, allows us to fully reconstruct the cell complex from the HSF structure.
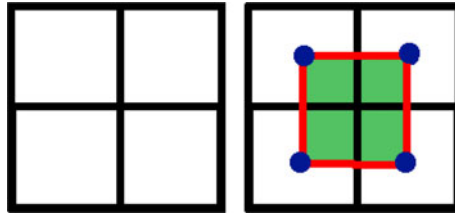
4.1 Cellular level

In order to propose a general topological framework for digital images in which most of their properties or features correspond to topological properties in $\mathbb{R}^n$, two main different types of methods have been developed in the literature: those based on the adjacency graph (see for instance [6, 25, 36, 39]) and those based on 2-dimensional cell complexes (see for example [23, 26, 28, 29, 41]). The method proposed here is a hybrid model in which the image is processed using and modifying a set of directed trees in the whole image. Any ASDR complex could be valid, and we can choose the most suitable one, depending on the application and the processing we want to execute.

First, we model in a semi-continuous way a topology of the Euclidean plane. To do this, and supposing that the $2D$ image is defined on a discrete set $D \subset \mathbb{R}^2$, the usual idea is that D is identified with the set of 2-cells of the complex and the lower-dimensional cells have to be generated additionally. In [27, 30], $D = \mathbb{Z}^2$ (standard case) is identified with the set of 2-cells of a uniform planar square cell complex $\mathcal{K}$, called Kovalevsky's cell complex.

We present here an extension of this technique, taking into account that the discrete carrier $D \subset \mathbb{R}^2$ is also the uniform square planar grid $\mathbb{Z}^2$. The Cellular Level consists in principle of a cell complex $\mathcal{L}$ simple homotopically equivalent to $\mathbb{R}^2$. Its construction starts with a cell complex $\tilde{\mathcal{K}}$ (equivalent to the Kovalevsky's cell complex $\mathcal{K}$) such that the points of D are the 0-cells of $\tilde{\mathcal{K}}$, its 1-cells are the segments connecting 4-adjacent points and its 2-cells are the squares having as corners to four mutually 8-adjacent points (see Fig. 8).

After that, triangular 2-cells connecting three mutually 8-adjacent points are added to $\tilde{\mathcal{K}}$. The intersection of each 2-cell c_t of this type with $\tilde{\mathcal{K}}$ is formed by two perpendicular 1-cells having in common a point of D. The third 1-cell belonging to the boundary of c_t is that joining two 8-adjacent diagonal points in D and it is a free edge (it belongs to only one 2-cell, that is, c_t). In this way, the triangular 2-cells add elementary "pockets" to $\tilde{\mathcal{K}}$ and specify the morphology of $\mathcal{L}$. The possible cell configuration for an object of interest in the subset $N_8 \subset D$ of any four points of

Fig. 8 A 2 × 2 digital image based on square pixel and its corresponding initial ASDR complex. 0-cells are colored in *blue*, 1-cells in *red* and 2-cell (*square*) in *green*

D mutually 8-adjacent are (up to isometry) shown in Fig. 9. The underlying idea behind the integration of a planar structure with elementary "pocket" defects at the cellular level is twofold: to automatically obtain optimal gradient vector fields for the ambiance space and to express all the previous point configurations suitably in terms of vectors at conceptual level.

Summing up, the Logical level has been determined in terms of a cell subcomplex of $\mathcal{L}$ In this schema, some geometric information (for example, diagonal edges) appears as elementary cellular perturbation of the topology of the Euclidean plane. This is the way in which Geometry is integrated in this topological schema. Notice that in practice, the cell complex $\mathcal{L}$, having four triangular micro-pockets for each square 2-cell in the plane, is the maximal (in terms of cells) ambiance cell complex in our framework. The next conceptual level for a digital image determine the concrete ambiance space, with each triangular pocket at cellular level specified by a corresponding diagonal arrow at conceptual level.

4.2 Conceptual level: tree-based homology information

The Conceptual Level briefly consists of installing homology information on terms of a HSF representation on a ASDR cell subcomplex $\mathcal{L}'$ of $\mathcal{L}$ and handling this information in a combinatorial way. More precisely, we manage and modify at a cell level, the vector space produced by the image of a chain homotopy operator describing the acyclicity of the cell complex $\mathcal{L}'$. In other words, we apply graph-based techniques for transforming a HSF representation of an image into another via local operations at conceptual level.

In order to develop a consistent and reusable framework for homology-based 2D digital image processing, we take advantage of an ambiance-based image processing

Fig. 9 Cell complex showing the four "pockets" corresponding to four mutually 8-adjacent points. The edges forming the triangular cells are: $((a, d), (d, c), (c, a))$, $((a, b), (b, d), (d, a))$ (in *red*) and $((a, b), (b, c), (c, a))$, $((c, b), (b, d), (d, c))$ (in *blue*)
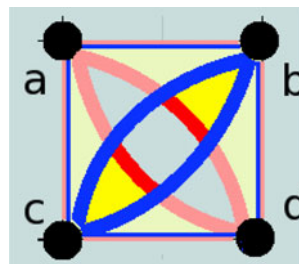
and the one-to-one mapping between HSF representations and optimal discrete gradient vector fields in ASDR cell complexes.

We subdivide this section into two parts: (a) Possible HSF-models for the square subdivided topological plane $\mathcal{L}$ with triangular micro-pockets; and (b) Local interchanging operations in the HSF-model of a digital image $I : D \to V$. From now on, taking into account that we work here with ASDR cell sub-complexes of $\mathcal{L}$, we identify optimal discrete gradient vector fields and its corresponding combinatorial chain homotopy operators (see Theorem 1) with HSF representations. These notions are suitably mixed in the following statements and results.

4.2.1 Homological initial state for the ambiance space

Let us install on the ASDR cell complex $\tilde{\mathcal{K}}$ defined in Section 4.1, an initial optimal gradient vector field $\mathcal{F}$. It is an easy task to create such vector field. In fact, it describes the acyclicity of the cell complex and can be identified with a HSF representation $\mathcal{F}$ of $\tilde{\mathcal{K}}$ (see Theorem 1). The construction of the HSF structure from the optimal gradient vector field has been detailed in the previous section. In Fig. 7, the forest $\mathcal{F}_1^{\mathcal{V}}$ is expressed in terms of the vector field $\mathcal{V}$ (in yellow) and the tree $\mathcal{F}_0^{\mathcal{V}}$ is colored in red (note that we have avoided the vertices of this last tree corresponding to the edges of $\tilde{\mathcal{K}}$, and therefore $\mathcal{F}_0^{\mathcal{V}}$ becomes a "spanning tree").

4.2.2 Local operations involving combinatorial chain homotopies

Using an ambiance-based approach, problems related to the "measurement" of topological phenomena (like holes or tunnels of a 3D digital image), can be solved in a satisfactory way. On the other hand, topological invariants (in particular, homology) are global characteristics of the object, and a consistent framework for topology-based image processing must give a quick and correct answer for extracting this topological information when an elementary local "deformation" is applied. We demonstrate here that some elementary local changes on the corresponding HSF representation, have an automatic translation to the global setting. These local changes are seen in terms of chain homotopy operators (or, equivalently, in terms of discrete vector fields) involving a reduced subset S of neighbors cells. In fact, the only constraint for S is that it must be closed by the concrete discrete vector field installed on $\mathcal{L}$. In $2D$ we put the emphasis on three types of HSF operations: (a) Arrow reversing (b) Edge Rotation and (c) Face Rotation. We do not give a proof here of the following results, that can be easily proven.

Algorithm 1 (Arrow Reversing) *Let $\mathcal{F} = \{T_1, T_2, \ldots, T_r\}$ be a HSF representation of an ASDR cell subcomplex of $\mathcal{L}$. Let c_0, c_0' be two 0-cells, such that c_0' is the sink vertex in $\mathcal{F}$ and there is a directed path p of 1-cells $c_0 : e_1, e_2, \ldots, e_n : c_0'$ in $\mathcal{F}$ from c_0 to c_0'. Then, we can construct a new HSF-representation $\mathcal{F}'$ that is identical to $\mathcal{F}$, except for the 0-cells belonging to the path p. In fact, the new pairs in the resulting HSF-representation are $\{c_0', e_n\}$ and those pairs from 0-cells to 1-cells in the directed path $c_0' : e_n, e_{n-1}, \ldots, e_1 : c_0$. In $\mathcal{F}'$, c_0 is the new sink vertex.*
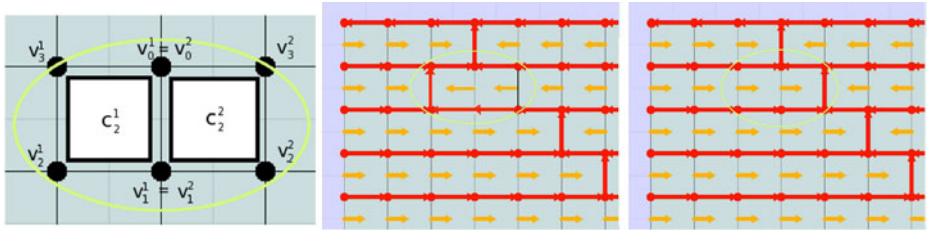
Fig. 10 Arrow reversing example where the *blue point* represents c_0 and the *green one* represents c_0'

In Fig. 10, an arrow-reversing operation is shown (see the path drawn in red). Arrow-reversing operations for 1-cells are not allowed due to the fact that each 1-cell that does not belong to the 1-forest $\mathcal{F}_1$ of the HSF $\mathcal{F}$ is paired with a 2-cell.

Algorithm 2 (Edge Rotation) *Let c_0 be a 0-cell, c_1 and c_1' be two 1-cells and c_2 a 2-cell of an ASDR cell subcomplex $\mathcal{L}'$ of $\mathcal{L}$. Let $\mathcal{F} = \{\mathcal{F}_0, \mathcal{F}_1\}$ be a HSF-representation of $\mathcal{L}'$ with associated combinatorial chain homotopy operator ϕ. Working at Conceptual Level, if $\{c_0, c_1\}$ is an arrow in the 0-tree $\mathcal{F}_0$, $\{c_1', c_2\}$ is an arrow in the 1-forest $\mathcal{F}_1$ and c_0, c_1 and c_1' belongs to the boundary of c_2, then we can generate a HSF-representation $\tilde{\mathcal{F}}'$ with associated combinatorial chain homotopy operator $\tilde{\phi}$ defined by $\tilde{\phi}(c) = \phi(c)$ for any cell c different from c_0 and c_1, $\tilde{\phi}(c_0) = c_1'$ and $\tilde{\phi}(c_1) = c_2$.*

In the Edge Rotation transformation, the underlying cellular structure can be modified. We can not guarantee that the final HSF representation belongs to the original cell complex $\mathcal{L}'$. In Fig. 11, we show some elementary examples of edge rotations.

Fig. 11 Edge rotation examples

Fig. 12 Face rotation example

Algorithm 3 (Face Rotation) *Let c_2^1 and c_2^2 two (both square or both triangular) 2−cells of an ASDR cell subcomplex $\mathcal{L}'$ of $\mathcal{L}$, sharing a common edge $e_1^1 = e_1^2$. Let $\mathcal{F}$ be a HSF representation of $\mathcal{L}'$ and ϕ an associated combinatorial chain homotopy operator. Working at Conceptual Level, if all the cells of the subcomplex $C(c_2^1, c_2^2)$ generated by the closures of c_2^1 and c_2^2 can be grouped by pairs of the gradient vector field $\mathcal{F}$, then we can generate a new acyclic combinatorial chain homotopy operator $\tilde{\phi}$. Using the labeling indicated in Fig. 12, its HSF representation $\tilde{\mathcal{F}}$ agrees with F excepting for the pairs of $C(c_2^1, c_2^2)$. For such pairs and for $i, j \in \{1, 2\}$ with $i \neq j$, $\{v_k^i, e_\ell^i\}$ belongs to a 0-tree of $\tilde{\mathcal{F}}$ if $\{v_k^j, e_\ell^j\}$ belongs to a 0-tree of $\mathcal{F}$ and $\{e_k^i, c_2^i\}$ belongs to a 1-tree of $\tilde{\mathcal{F}}$ if $\{e_k^j, c_2^j\}$ belongs to a 1-tree of $\mathcal{F}$ (see Fig. 12).*

Let $I : D \to R$ be a digital image with an 8-connected object of interest $O \in D$. Then, it is possible to modify an initial HSF representation (and its corresponding combinatorial chain homotopy operator) by means of the previous local operations, in such a way that the result is a new HSF representation, called HSF-representation of I based on O, in which a finite set of edges (called *bridge edges*) link the object of interest with the background.

This homology-based transformation is processed in two steps: (a) for each pixel in the inner boundary of O (that is, belonging to O and having a pixel not in O as 8-neighbor) we select, if possible, an arrow connecting this pixel with other neighbor pixel of the inner boundary of O (by using an elementary edge rotation); (b) for each
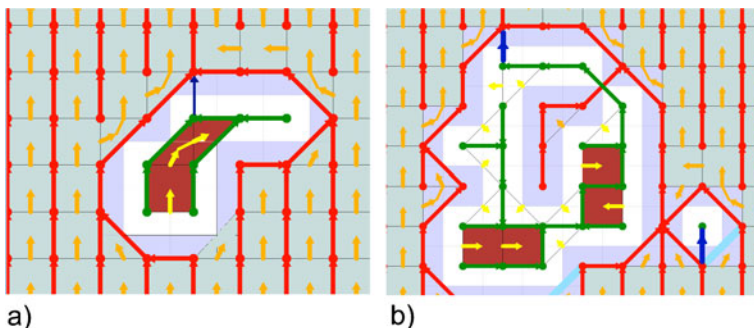

**Fig. 13** Examples of HSF-representation based on objects of interest

pixel in the outer boundary of O (that is, belonging to the complementary of O and having a pixel in O as 8-neighbor) we select, if possible, an arrow connecting this pixel with other neighbor pixel of the outer boundary of O (by using an elementary edge rotation). At the end of this process, we have almost "isolated" (along its crack) the object O from the background, excepting the existence of a set of edges in the new HSF representation, called bridge edges, that connect O with its complementary. In Fig. 13, some HSF-representations based on an object of interest are shown.

5 Homology and cohomology of objects of interest

Let $I : D \rightarrow R$ be a 2D digital image and $O \in D$ be a (non-necessarily 8-connected) object of interest. Let $\mathcal{F} = \{\mathcal{F}_0, \mathcal{F}_1\}$ be a HSF representation based on O and $\phi : L \rightarrow \mathbb{Z}/2\mathbb{Z}[L']$ be its corresponding acyclic combinatorial chain homotopy operator over an ASDR cell subcomplex L' of L. It is possible to deduce homology groups and generators of the cell subcomplex $L(O) \subset L$ generated by the pixels of O (it is called the homology of O with coefficients in $\mathbb{Z}/2\mathbb{Z}$) from the HSF representation $\mathcal{F}$. In other words, the 8-connected components and holes of the object of interest can be easily determined from this HSF representation. In other words, it is possible to deduce a HSF representation for a digital object from one of the ambiance space, by doing some minor local modifications (Fig. 14).

The idea is to consider the sub-forest $\mathcal{F}'$ of the forest $\mathcal{F}$, corresponding to the subcomplex $L(O)$ (that is, the HSF representation of the object O).

Fig. 14 Example of HSF representation based on two ROIs (set of black pixels in the image). The 0-tree is represented by a spanning tree and the 1-tree of the HSF structure is determined by a vector field
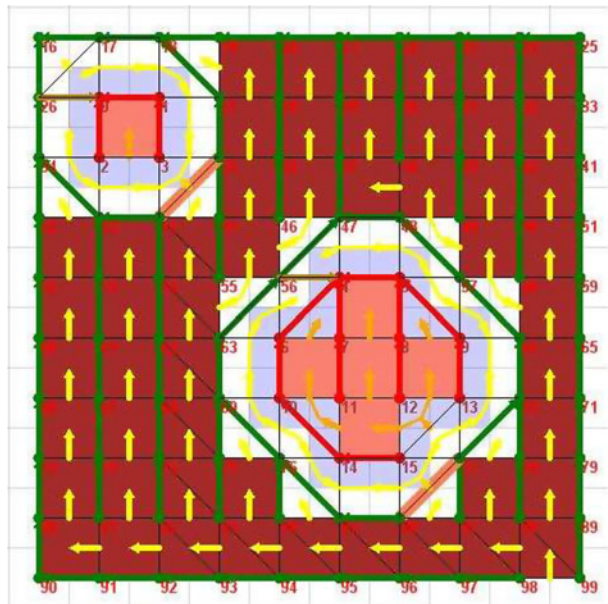
Let us denote $\mathcal{F}' = (T_{1,1}, \ldots T_{1,n_1}, T_{2,1}, \ldots T_{2,n_2})$, where $T_{1,*}$ are 0-trees (with $* \in \{1, \ldots, n_1\}$) of $\mathcal{F}'$ and $T_{2,*}$ are 1-trees (with $* \in \{1, \ldots, n_2\}$) of $\mathcal{F}'$. Let us suppose that the sink s is not in O. Then, the following results hold:

(a) the (unpaired) vertices in O (also called critical vertices) are representative cycle generators of the corresponding connected components of O. Therefore c is the number of connected components in O.

(b) any unpaired 1-cell (u, v) (also called critical edge) gives rise to a 1-homology generator fitting geometrically with the outer or some inner boundary of O. In fact, this homology cycle is obtained by the formula $\{u, v\} + \phi(u) + \phi(v)$. If the complementary of O has h connected components (including background), the number of critical edges is $h - 1$. Associated to each critical edge, there is a 1-tree of $\mathcal{F}'$. The number of 1-cells corresponding to critical edges of a 1-tree of $\mathcal{F}'$ can be greater than one.

Each critical edge can be "moved" along its associated tree $T_{m,n}$, in order to get different representative cycles of the corresponding 1-homology generator. This translation of the critical edge can be done using reversing-arrow operations. It is clear that a HSF-representation based on an object of interest O is also suitable for obtaining homology information about the complementary of O.

In Fig. 15 two different HSF representations of an object of interest are shown. The black edge represents the 1-homology generator of the hole in the object. The homology cycle is colored in blue.
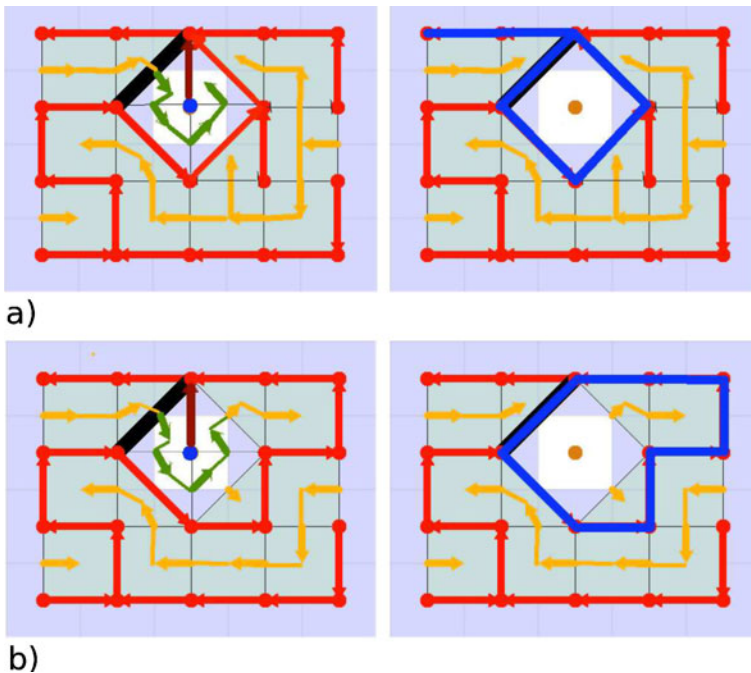

a)

b)

Fig. 15 Two different examples of HSF-representations and the resulting homology generator (in *blue*) computed for the same object of interest

Moreover, we can easily deal with cohomology information starting from a HSF representation of an object. For example, the tree $T_{\{u,v\}}$ associated to each critical edge (u, v) determines in a straightforward manner a representative cocycle c_T of a cohomology generator of dimension 1. This cochain $c_T : \{1 - cells \in L(O)\} \to \mathbb{Z}/2\mathbb{Z}$ is not null only for the vertices (that is, the 1-cells of $L(O)$) belonging to the tree $T_{u,v}$. In Fig. 16 we show how cohomology can be equivalent to a type of paths in the HSF representation such that if we "cut" the object through this path, the resulting object has one hole less than before.

We have asserted in the abstract that the HSF framework produces algorithmic answers to certain problems related to the homological classification of cycles (i.e., a sum of cells having zero boundary). The main important ones in the area of discrete image processing are the shortest cycle, contractibility and transformability problems. The shortest cycle problem is a generalization of the well-known shortest path problem [8] and can be stated as follows: Given a cycle c on a cell complex version K of a ROI, what is the shortest cycle on K homologically equivalent to it? The contractibility problem consists of checking wether a cycle can be contracted to a point and the transformability problem analyses wether two cycles can be transformed into each other. These problems have significant connections with another in computational topology: to determine the fundamental group of K or, equivalently, to construct a polygonal schema (cut a closed genus g surface to a canonical polygon with $4g$ edges). The work of Gouillard [19] gives a very complete account of the state of the art about these questions, treating them under a homotopical perspective.

We limit ourselves to demonstrate that contractibility and transformability problems can be automatically solved using the chain contraction $(f_{F_K}, g_{F_K}, \phi_{F_K})$ canonically associated to an HSF structure F_K of a ROI K.

Given a contractible q-cycle c on K, then we have:

$$c + g_K f_K(c) = \partial_K \phi_K(c) + \phi_K \partial_K(c)$$

Since $\partial_K(c) = 0$ (c is a cycle) and $f_K(c) = 0$ (because c is contractible and its associated homology generator is zero), we reduce the previous equality into the following one:

$$c = \partial_K \phi_K(c)$$

That means, that $\phi_K(c)$ is the $(q + 1)$-chain whose boundary is c (Fig. 17).
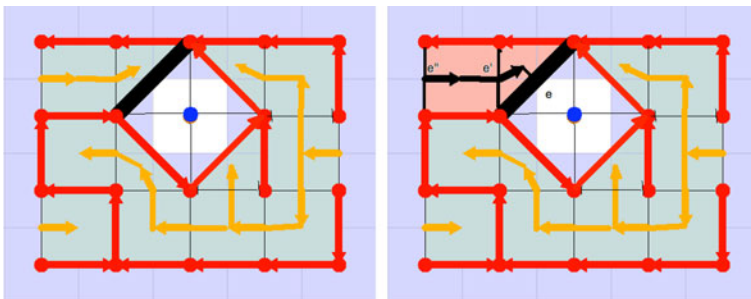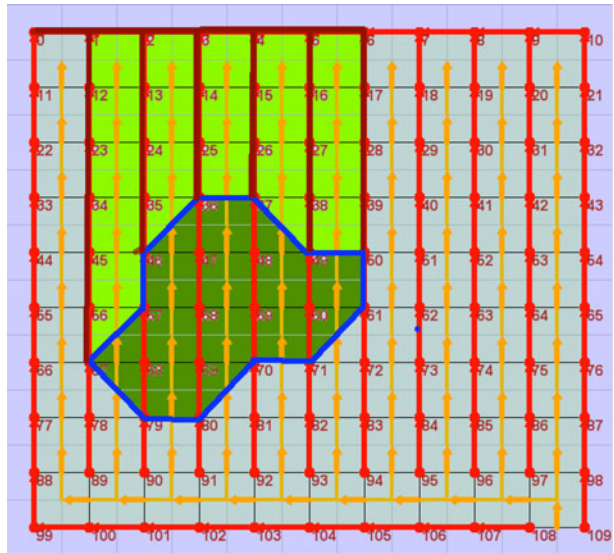

Fig. 16 A HSF-representation (on the *left*) and the path (on the *right* picture, in *black*) representing cohomology

Fig. 17 An acyclic scenario, one cycle c in *blue*, and the corresponding sum of 2-cells $\phi_K(c)$ in strong *green* color

Given now two q-cycles homologically equivalent c and c', then:
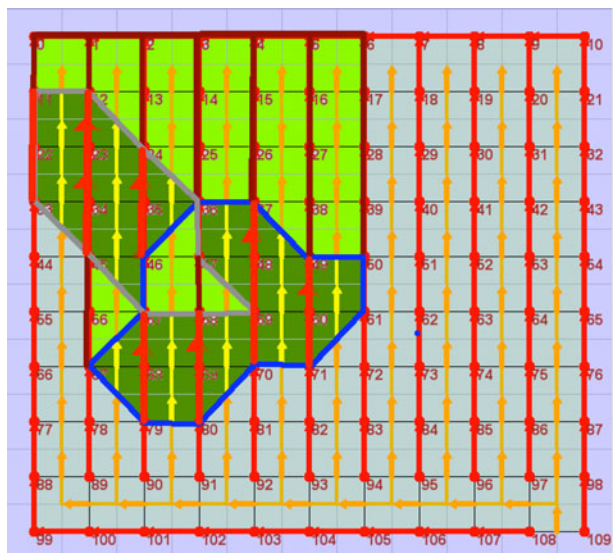
$$c + g_K f_K(c) = \partial_K \phi_K(c)$$

$$c' + g_K f_K(c') = \partial_K \phi_K(c')$$

If we subtract one equation from another, we have:

$$c + c' = \partial_K \phi_K(c - c')$$

Fig. 18 A simple scenario of acyclic ambiance, two cycles c and c' in *blue* and *grey*, respectively and the sum of 2-cells composing $\phi_K(c + c')$ in strong *green* color

due to the fact that $g_K f_K(c) = g_K f_K(c')$. That means that $\phi_K(c + c')$ is the $(q + 1)$-chain whose boundary is the difference between the original cycles (Fig.18).

6 Parallel homology-based processing

Within this context of homology-based processing, it is possible to exploit data parallelism. Although the methods designed here open the possibility to a parallel processing, we are still far from devising a realistic and practical parallel approach.

Being n the number of pixels or 0-cells in L, the idea is to decompose the cell complex L into n subsets of cells, each of them included into the neighborhood of a concrete vertex.

We consider as many Processing Elements (PE) as pixels the image has. A PE(v) in this architecture consists of a subset E of cells having a pixel v with integer coordinates (x, y) as element of its boundary. More concretely:

$$E = \big\{ \{(x, y)\}, \{(x, y), (x - 1, y + 1)\}^+, \{(x, y), (x - 1, y + 1)\}^-, \{(x, y), (x + 1, y)\},$$
$$\{(x, y), (x - 1, y), (x - 1, y + 1)\}, \{(x, y), (x - 1, y + 1), (x, y + 1)\},$$
$$\{(x, y), (x, y + 1)\}, \{(x, y), (x + 1, y + 1)\}^+, \{(x, y), (x + 1, y + 1)\}^-,$$
$$\{(x, y), (x, y + 1), (x + 1, y + 1)\}, \{(x, y), (x + 1, y), (x + 1, y + 1)\},$$
$$\{(x, y), (x + 1, y), (x + 1, y + 1), (x, y + 1)\} \big\}$$

where $(x, y)^{\pm}$ indicates the respective upper $(+)$ and lower $(-)$ diagonal edges.

In order to clarify this idea, a PE is shown on the left image of Fig. 19. The pixel P is represented in green, the six 1-cells in blue, the four triangular-like 2-cells in yellow, and the one square 2-cell in orange.

As it is shown in the middle image of Fig. 19, we consider that the cells $\{(x, y), (x - 1, y + 1)\}^-$ and $\{(x, y), (x - 1, y), (x - 1, y + 1)\}$ are always paired.

Given a pixel which is not the sink, the task consists of pairing the vertex P with an edge of E, being paired the rest of cells in E in a straightforward manner. For example, if we pair P with the edge $\{(x, y), (x - 1, y + 1)\}^+$, then the pairing of the rest of cells is (see right image of Fig. 19):

$$\big\{ (\{(x, y), (x, y + 1)\}, \{(x, y), (x - 1, y + 1), (x, y + 1)\}),$$
$$(\{(x, y), (x + 1, y + 1)\}^+, \{(x, y), (x, y + 1), (x + 1, y + 1)\}),$$
$$(\{(x, y), (x + 1, y + 1)\}^-, \{(x, y), (x + 1, y), (x + 1, y + 1)\}),$$
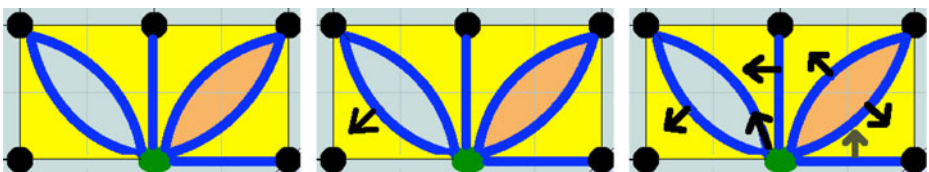$$(\{(x, y), (x + 1, y)\}, \{(x, y), (x + 1, y), (x + 1, y + 1), (x, y + 1)\}) \big\}$$

Fig. 19 A PE on the *left* and a pairing example on the *right*

This procedure is specified in the following algorithm:

Algorithm 4 (Parallel optimal discrete gradient vector field) *$PE(v)$ is a unit processing element "centered" at pixel v.*
> *for each $PE(v)$ parallel do*
>> *Choose one edge e having as source the vertex v.*
>> *Establish the pair $\{v, e\}$.*
>> *Pair the rest of incident edges and 2-cells in $PE(v)$.*
> *end*

Taking n processors (as many as pixels the image has), the speedup S_n, measuring how much the parallel algorithm of establishing a random acyclic combinatorial chain homotopy operator ϕ is faster than the corresponding sequential algorithm, is ideal. That means that $S_n = \frac{n}{1} = n$ and its efficiency is 1. We suppose here that the sink of ϕ is always a priory known pixel.

7 Conclusions

Several applications in digital imagery are in need of a flexible and topologically-consistent framework for nD object analysis and recognition. We have presented here a new 2D digital image processing framework based on chain homotopies determining an advanced topological analysis of cell complexes. The main notion in this framework is called Homological Spanning Forest (or HSF, for short) for a digital object due to the fact that it can be considered as a suitable generalization to higher dimensional cell complexes of the topological meaning of a spanning tree of a geometric graph. This new model for a digital object O is a set of directed forests, which can be constructed under an underlying cell complex format $K(I)$ of the image. Taken as initial data, a 2D digital image I and a set of ROIs $R_1, R_2, \ldots, R_t$ previously determined by means of an image processing algorithm, we follow the sequence:

(1) To construct an initial HSF representation for a whole 2D digital image I that is independent of the pixel contents of it and that "suits" well with the concrete task we want to do.
(2) To construct a new HSF configuration "adapted" to the ROIs, from which new HSF structures for the last ones can be almost automatically obtained and a subsequent topological analysis of them can be done.

This schema focus on transforming conceptual level information starting from relevant logical level knowledge. It is also possible to deduce new logical level structures from the data at pixel level, remaining "untouched" the HSF system that is fixed at the very beginning. In this case, the result at conceptual level could be interpreted in highly hierarchical terms (quad-trees, pyramids,...).

In the immediate future, we have the intention of progressing to the following directions:

(a) A short-term objective is to extend this method to higher dimensions. This would allow a fast topological-controlled processing of big images like for example medical 4D images. Whereas the study of 2D and 3D digital images has been very fruitful, in the study of 4D-phenomena many research questions

related to the topology are still fully open. 4D-images analysis is an important next step, because it adheres to the dimensionality of what is the physical reality. We also intend to achieve parallelism in this context.

(b) The application of the HSF schema brings many advantages for fast geometrical transformations of images, and for implementing flexible and reliable methods for structural image analysis (see for instance [12]). Depending of the application we want to deal with, it seems possible to modulate the potential full flexibility of the proposed framework, in such a way that its conceptual description would be suitable for a concrete topological task (skeletons, thinning, Reeb graphs, mathematical morphology, etc).

(c) To integrate in the HSF framework persistence homological techniques [9], discrete differential forms methods [7] and Morse Homology descriptors [1].

(d) A carefully study about cycle transformability questions and others related to relative homology and advanced algebraic topological information (cohomology algebra, homology A(∞)-coalgebra, cohomology operations,....) in 3D or 4D HSF context will also be done in a future work. The computational homological algebra framework developed in [34] for HSF operators will be essential for advancing in this area.

References

1. Allili, M., Corriveau, D.: Topological analysis of shapes using Morse theory. Comput. Vis. Image Underst. **105**, 188–199 (2007)
2. Ankeney, L.A., Ritter, G.X.: Cellular topology and its applications in image processing. Int. J. Parallel Program. **12**, 433–456 (1983)
3. Ayala, R., Domínguez, E., Francés, A.R., Quintero, A.: Determining the components of the complement of a digital (n-1)-manifold in $\mathbb{Z}^n$. In: Proceedings of the 6th International Workshop on Discrete Geometry for Computer Imagery, pp. 163–176. Springer-Verlag, London, UK (1996)
4. Bertrand, G., Couprie, M.: On parallel thinning algorithms: minimal non-simple sets, p-simple points and critical kernels. J. Math. Imaging Vis. **35**, 23–35 (2009)
5. Cardoze, D., Miller, G., Phillips, T.: Representing topological structures using cell-chains. In: Geometric Modeling and Processing, pp. 248–266. Pittsburgh, PA (2006)
6. Chassery, J.M.: Connectivity and consecutivity in digital pictures. Comput. Graph. Image Process. **9**(3), 294–300 (1979)
7. Desbrun, M., Kanso, E., Tong, Y.: Discrete differential forms for computational modeling. In: ACM SIGGRAPH 2005 Courses, SIGGRAPH '05. ACM, New York, NY, USA (2005)
8. Dijkstra, E.W.: A note on two problems in connexion with graphs. Numer. Math. **1**, 269–271 (1959)
9. Edelsbrunner, H., Letscher, D., Zomorodian, A.: Topological persistence and simplification. In: Proceedings of the 41st Annual Symposium on Foundations of Computer Science, pp. 454–463. IEEE Computer Society, Washington, DC, USA (2000)
10. Eilenberg, S., Mac Lane, S.: On the groups $H(\pi, n)$, i, ii, iii. Ann. Math **58, 60, 60**, 55–106,48–139, 513–557 (1953,1954)
11. El-Kwae, E.A., Kabuka, M.R.: Binary object representation and recognition using the Hilbert morphological skeleton transform. Pattern Recogn. **33**(10), 1621–1636 (2000)
12. Feichtinger, H.G., Onchis, D.M.: Constructive realization of dual systems for generators of multi-window spline-type spaces. J. Comput. Appl. Math. **234**, 3467–3479 (2010)
13. Forman, R.: A discrete Morse theory for cell complexes. In: Yau, S.T. (ed.) Geometry, Topology and Physics for Raoul Bott. International Press (1995)

14. Forman, R.: Morse theory for cell complexes. Adv. Math. **134**, 90–145 (1998)
15. González-Diaz, R., Jiménez, M., Medrano, B., Molina-Abril, H., Real, P.: Integral operators for computing homology generators at any dimension. In: Ruiz-Shulcloper, J., Kropatsch, W. (eds.) Progress in Pattern Recognition, Image Analysis and Applications. Lecture Notes in Computer Science, vol. 5197, pp. 356–363. Springer Berlin/Heidelberg (2008)
16. González-Díaz, R., Jiménez, M.J., Medrano, B., Real, P.: Chain homotopies for object topological representations. Discrete Appl. Math. **157**(3), 490–499 (2009)
17. González-Díaz, R., Jiménez, M.J., Medrano, B., Real, P.: A tool for integer homology computation: λ-AT-model. Image Vis. Comput. **27**(7), 837–845 (2009)
18. González-Díaz, R., Real, P.: On the cohomology of 3d digital images. Discrete Appl. Math. **147**(2–3), 245–263 (2005)
19. Gouaillard, A.: Contexte générique bi-multirésolution basé ondelettes pour l'optimisation d'algorithmes de surfaces actives. Ph.D. thesis, Inst. National des Sciences Appliquées de Lyons (2005)
20. Gugenheim, V.K.A.M., Lambe, L.A., Stasheff, J.D.: Perturbation theory in differential homological algebra. Ill. J. Math **33**, 357–373 (1989)
21. Gugenheim, V.K.A.M., Lambe, L.A., Stasheff, J.D.: Perturbation theory in differential homological algebra. ii. Ill. J. Math. **35**(3), 357–373 (1991)
22. Kaczynski, T., Mrozek, M., Slusarek, M.: Homology computation by reduction of chain complexes. Comput. Math. Appl. **35**(4), 59–70 (1998)
23. Khalimsky, E.: Pattern analysis of *n*-dimensional digital images. In: Proc. IEEE Int. Conf. Systems, Man and Cybernatics, pp. 1559–1562 (1986)
24. Klette, R.: Cell complexes through time. In: Latecki, L.J., Mount, D.M., Wu, A.Y. (eds.) Proc. Vision Geometry IX, vol. 4117, pp. 134–145 (2000)
25. Klette, R., Rosenfeld, A.: Digital Geometry: Geometric Methods for Digital Picture Analysis. Morgan Kaufmann Series in Computer Graphics (2004)
26. Kong, T.Y., Kopperman, R., Meyer, P.R.: A topological approach to digital topology. Am. Math. Mon. **98**, 901–917 (1991)
27. Kovalevsky, V.: Finite topology as applied to image analysis. Comput. Vis. Graph. Image Process. **46**, 141–161 (1989)
28. Kovalevsky, V.: Algorithms in digital geometry based on cellular topology. Lect. Notes Comput. Sci. **3322**, 366–393 (2005)
29. Kovalevsky, V.: Axiomatic digital topology. J. Math. Imaging Vis. **26**, 41–58 (2006)
30. Kovalevsky, V.: Geometry of Locally Finite Spaces. House Dr. Baerbel Kovalevski (2008)
31. Kropatsch, W.G., Haxhimusa, Y., Ion, A.: Multiresolution image segmentations in graph pyramids. In: Kandel, A., Bunke, H., Last, M. (eds.) Applied Graph Theory in Computer Vision and Pattern Recognition. Studies in Computational Intelligence, vol. 52, pp. 3–41. Springer (2007)
32. Lienhardt, P.: Topological models for boundary representation: a comparison with n-dimensional generalized maps. Comput.-Aided Des. **23**(1), 59–82 (1991)
33. Molina-Abril, H., Real, P.: Homological computation using spanning trees. In: CIARP 2009. Lecture Notes in Computer Science, vol. 5856, pp. 272–278 (2009)
34. Molina-Abril, H., Real, P.: Towards optimality in discrete Morse theory through chain homotopies. In: CTIC 2010, Imagen-a, vol. 1, pp. 33, 40 (2010)
35. Molina-Abril, H., Real, P.: Homological optimality in discrete Morse theory through chain homotopies. Pattern Recog. Lett. (2012). doi:10.1016/j.patrec.2012.01.014
36. Parker, J.: Algorithms for Image Processing and Computer Vision. Wiley, New York (1997)
37. Romero, A., Sergeraert, F.: Discrete vector fields and fundamental algebraic topology. CoRR **abs/1005.5685** (2010)
38. Romero Rodríguez, B., Falces Sánchez, J.: Homología y Arboles Recubridores. Master's thesis, E.T.S. Ingeniería Informática, Universidad de Sevilla, Spain (2009)
39. Rosenfeld, A.: Connectivity in digital pictures. J. Assoc. Comput. Mach. **17**(1), 146–160 (1970)
40. Sergeraert, F.: The computability problem in algebraic topology. Adv. Math. **104**, 1–29 (1994)
41. Webster, J.: Cell complexes and digital convexity, pp. 272–282. Springer, New York (2001)
42. Whitehead, J.: Combinatorial homotopy i. Bull. Amer. Math. Soc. **55**, 213–245 (1949)